NASA Technical Memorandum 81359

A Comparison of Laboratory Measured Temperatures With Predictions for a Spar/Skin Type Aircraft Structure

Jerald M. Jenkins

May 1981

NASA

NASA Technical Memorandum 81359

A Comparison of Laboratory Measured Temperatures With Predictions for a Spar/Skin Type Aircraft Structure

Jerald M. Jenkins
Dryden Flight Research Center
Edwards, California

National Aeronautics and
Space Administration

1981

A Comparison of Laboratory Measured Temperatures with Predictions for a Spar/Skin Type Aircraft Structure

Jerald M. Jenkins
Dryden Flight Research Center

INTRODUCTION

As new computational tools become available there is frequently a significant time period before the analytical capability is compared to experimental data. The results of the heat transfer feature of the NASTRAN (reference 1) computer program have not been extensively applied to measured thermal data. The contents of this paper provide some insight into the usefulness of this particular calculative tool. A typical aircraft type of structure with spar/skin type of construction is partially heated for a significant time period. The structure conducts, radiates, and convects freely so that a fairly complicated laboratory test situation is created. A NASTRAN thermal model is developed, temperatures are calculated, and temperature calculations are compared to laboratory measured temperatures.

SYMBOLS

C_p	specific heat, J/kg-K° (BTU/lb-F°)
h	convective film coefficient, J/s-m^2 (BTU/s-in^2)
i, j	first and second numbers, consecutively
k	thermal conductivity, J/s-m (BTU/s-in)

ε	emissivity
ρ	density, kg/m^3 (lb/in^3)

TEST STRUCTURE

A test structure with the cross-section properties shown in figure 1 was used for a heating experiment. The length of the specimen was 2.44 meters (96 inches). The skin was attached to zee-shaped spars using mechanical fasteners. A lower cap was attached to the bottom of the zee-shaped spars with mechanical fasteners. The skin was fabricated of 2024 aluminum in the T3 condition. The zee-shaped spars and the lower caps were fabricated of 6Al-4V titanium.

INSTRUMENTATION

The test structure was extensively instrumented with Chromel-Alumel thermocouples to measure structural temperatures. A bottom view of the test structure is presented in figure 2 showing many of the thermocouples. Measurements were taken on the spar side of the skin, the upper spar caps, the spar webs, and the lower spar caps.

TEST PROCEDURE

The heating test plan was to heat the upper surface (see figure 3) of the skin using radiant heaters. The lower part of the structure was shielded from the radiant heat. The skin was heated to 533 °K (500 °F) according to the time-history shown in figure 4. The specimen was heated with the skins in a horizontal position with the spars down. The ends and bottom of the specimen were open so that it could convect freely. The specimen was unpainted and the surface condition of the metal was as received from the manufacturer.

ANALYSIS

Thermal Model

The computational efforts in this paper are directed toward evaluating the heat transfer feature of the NASTRAN (reference 1) computer program. A three-dimensional model of a small portion of the center of the test structure was used for analysis. The basic conduction model was formed of CHEXA2 elements as shown in the cross-sectional representation in the upper part of figure 5. This

model has a length of .203 meters (8 inches). A time-history of temperature was applied to the model through the grid points located on the upper surface of the skin. This constituted the approach to the basic conduction model.

Radiation elements were added to the model as shown in the lower part of figure 5. The view factors used for the two small outer bays are identical and the view factors used for the three inner bays are the same. The values used in the radiation matrix (RADMTX) can be obtained by correlating the numbers of the radiation elements in figure 5 to the area-view factor products in figure 6. The values of the view factors were obtained from tables and charts in references 2 and 3. These values were then adjusted so that all the area-view factor products divided by the area of the element were numerically close to 0.99. This was done so that energy lost to space (a specific characteristic of NASTRAN) was minimized. The openings (side and bottom) were closed with radiation closure elements on the model so that nearly all of the radiation exchanges were accountable. An additional parameter greatly affecting the radiation heat transfer is the condition of the surface of the metal which leads to the value for the emissivity, ε. A correct value for the emmissivity is critical to the accuracy of the calculation.

Convection elements were included to simulate the losses from the vertical elements (spars) of the test structure. Convective heat transfer is, in general, a very complicated phenomenon. This experiment provides no exception since the local circulation of air in the proximity of the surfaces is a function of many variables. The primary tool for adjusting to this circulation with NASTRAN is through the convective film coefficient, h.

Analysis Sets

Since published experiences with the heat transfer part of NASTRAN are quite limited, the analytical work was approached in several logical steps. First, calculations of structural temperatures were made with only conduction heat transfer. Then radiation and convection were added to the problem in steps with perturbations of radiation geometry, emissivity, and convective film coefficient defining a group of analysis sets. The following sections will define the analysis sets in detail.

Analysis Set 1.- Temperatures at the grid points representing the upper surface of the skin were input to the problem in the form of a time-history identical to the laboratory skin heating of the test specimen. The CHEXA2 elements were allowed to conduct only. A thermal conductivity (k) value of 91.33 joules/second-meter (2199×10^{-6} BTU/second-inch) was used for the aluminum elements

and a value of 4.82 joules/second-meter (116 x 10^{-6} BTU/second-inch) was used for the titanium elements. A thermal capacity value (ρC_p) of 2.67 x 10^6 joules/degree kelvin-meter^3 (.023 BTU/degree Fahrenheit-inch^3) was used for the aluminum elements and a value of 2.41 x 10^6 joules/degree kelvin-meter^3 (.0208 BTU/degree Fahrenheit-inch^3) was used for the titanium elements.

Analysis Set 2.- The conduction process is augmented by radiation interchange between the lower skin surface elements and the spar elements. Radiation to space (a characteristic feature of NASTRAN) is allowed in the five unclosed bays. An emissivity of 0.9 was used.

Analysis Set 3.- Conduction and radiation are used in this set, however, non-conducting solid elements are added such that the five bays are closed. The view factor matrix is adjusted so that radiation losses to space are minimum and the solid elements are maintained at room temperature like the laboratory floors and walls. An emissivity of 0.9 was used.

Analysis Set 4.- Conduction and radiation with solid closure elements are used and convection heat losses from the spar elements are allowed. A value of 4.42 joules/second-meter^2-degree kelvin (1.5 x 10^{-6} BTU/second-inch^2-degree Fahrenheit) was used for the convective film coefficient. An emissivity of 0.9 was used.

Analysis Set 5.- Conduction and radiation with solid closure elements are used and larger (than Analysis Set 4) convection heat losses from the spar elements are allowed. A value of 5.59 joules/second-meter^2-degree kelvin (1.9 x 10^{-6} BTU/second-inch^2-degree Fahrenheit) was used for the convective film coefficient. An emissivity of 0.9 was used.

Analysis Set 6.- Conduction and radiation with the solid closure elements are used and convection heat losses from the spar elements are allowed. The same convective film coefficient as in the previous set was used. A reduced emissivity value of 0.64 was used.

RESULTS AND DISCUSSION

Laboratory measured temperatures at five spar locations are represented in figure 7 by the circular symbols. The data are presented as a time-history for the forty minute test. The data are compared to the temperatures calculated using Analysis Set 6. As can be seen, the calculated data compare closely to the measured

data. Some lag is seen in the early part of the test in figures 7(c) and 7(d). This is attributed to the fact that the conduction elements are more numerous than the radiation and convection elements in the spars. Hence, the grid points for the radiation and convection elements overlie the conduction elements and a resulting overshoot in heat loss occurs at some of the grid points. This causes premature radiation and convection losses at some grid points due to the coarseness of the radiation and convection representations. This anomaly would be eliminated by a larger number of radiation and convection elements.

Several measured temperature (circular symbols) distributions are shown in figure 8 for three different time segments (ten minutes, twenty minutes, and forty minutes). The measured data are compared to the values calculated using Analysis Set 6. The lag discussed in the previous paragraph is seen in figure 8(a). This effect is seen to dissipate in figure 8(b) and 8(c) as the conduction heat transfer begins to dominate the middle and lower elements of the model of the spar. The comparison of the measured and the calculated values is quite close at the forty minute time slice.

All six analysis sets are compared to the laboratory measured data in figure 9 for the time slice of forty minutes. It can be seen that the calculated values are high and have a large gradient from top to bottom of the spar for conduction only (Analysis Set 1). The addition of radiation (Analysis Sets 2 and 3) lessens the gradient and it can be seen that the closure elements raise the temperature. The addition of convection (Analysis Sets 4 and 5) lowers the temperatures significantly and the larger convective film coefficient case is seen to be fairly close to the experimental data. The last iteration (Analysis Set 6) illustrates the importance of the emissivity assumption. When the emissivity is changed from 0.9 to 0.64, the data are found to correlate extremely well.

There are several results that are of particular interest. The use of NASTRAN is particularly convenient for heat transfer if the ultimate goal is to achieve a structural analysis since it is practical to use common grid points and elements. Acceptable results were obtained without varying several thermal properties with temperature. The temperature variation of these parameters was apparently not large enough to affect the predicting capability for the range of temperatures in the test. Both radiation and convection modes of heat transfer are significant effects for this type of test with this type of structure. Assuming these two modes of heat transfer to be negligible would be a poor assumption.

CONCLUDING REMARKS

A typical spar/skin aircraft structure was heated non-uniformly in a laboratory and the resulting temperatures were measured. The heat transfer function of the NASTRAN computer program was used to provide predictions. The measured and calculated data were compared.

Calculated temperatures based on a thermal model with conduction, radiation, and convection features compared closely to measured spar temperatures. Acceptable results were obtained without varying the thermal conductivity, specific heat, or emissivity with temperature since the range of temperature variations was not large. All modes of heat transfer (conduction, radiation, and convection) were shown to significantly affect the magnitude and distribution of structural temperatures.

Dryden Flight Research Center
National Aeronautics and Space Administration
Edwards, Calif., April 20, 1981

REFERENCES

1. McCormick, Caleb W., ed.: The NASTRAN User's Manuel (Level 15). NASA SP-222(01), 1972.
2. Jakob, Max; and Hawkins, George A.: Elements of Heat Transfer and Insulation. Second ed., John Wiley & Sons, Inc., c.1950.
3. Rohsenow, Warren M.; and Hartnett, James P.: Handbook of Heat Transfer. McGraw-Hill Book Co., c.1973.

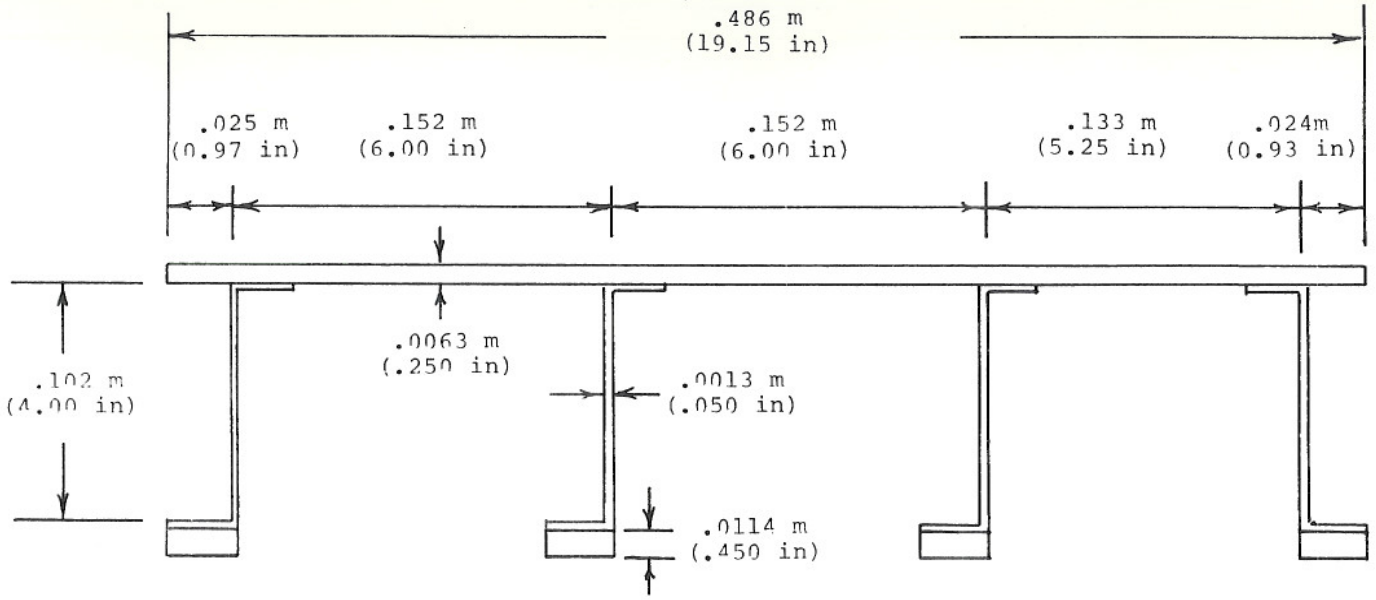

Figure 1. Cross-section dimensions of test specimen.

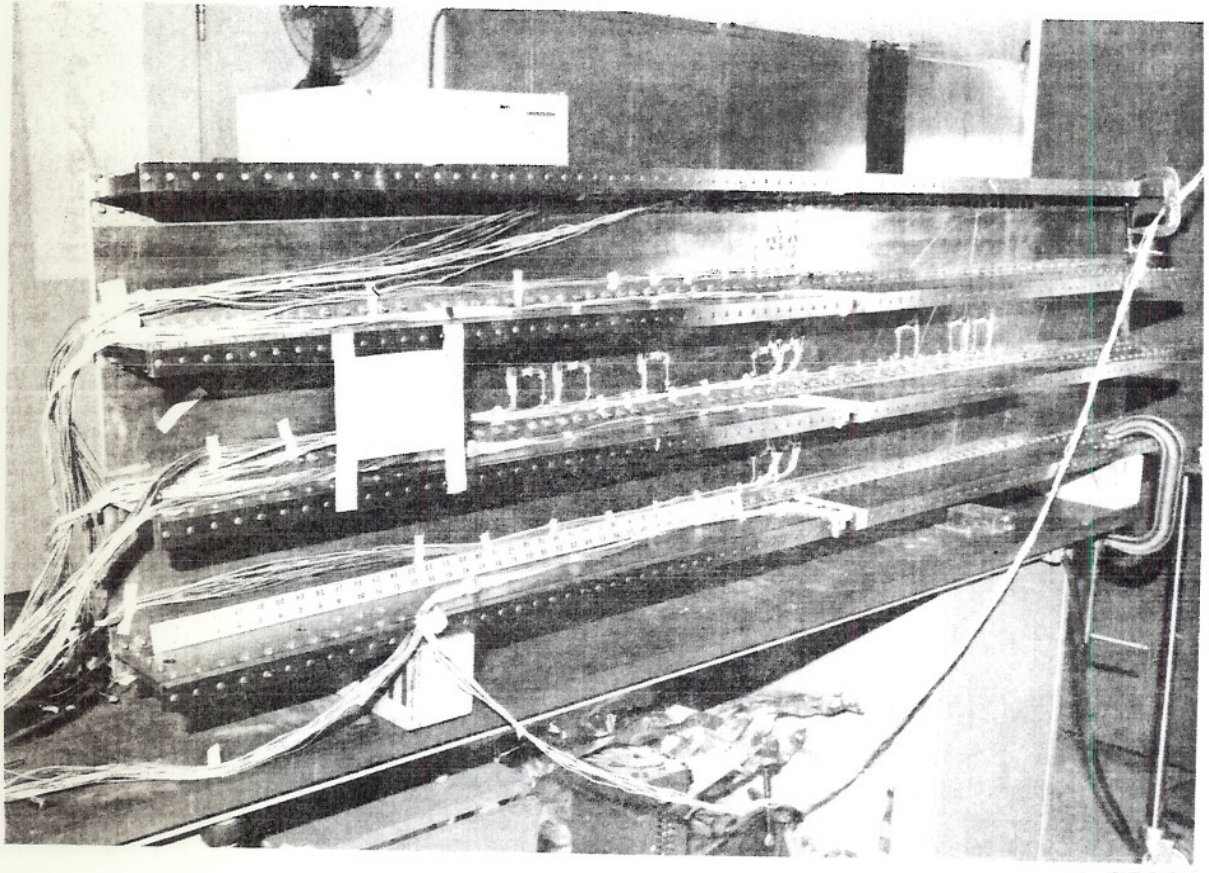

E-37838

Figure 2. Bottom view of test specimen showing instrumentation.

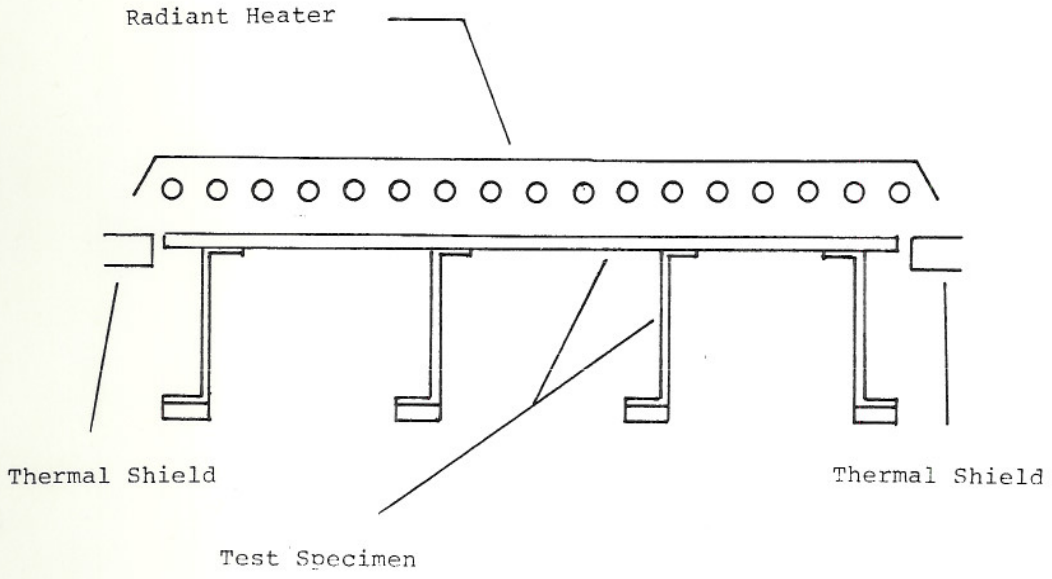

Figure 3. Sketch of test set-up illustrating the heating technique.

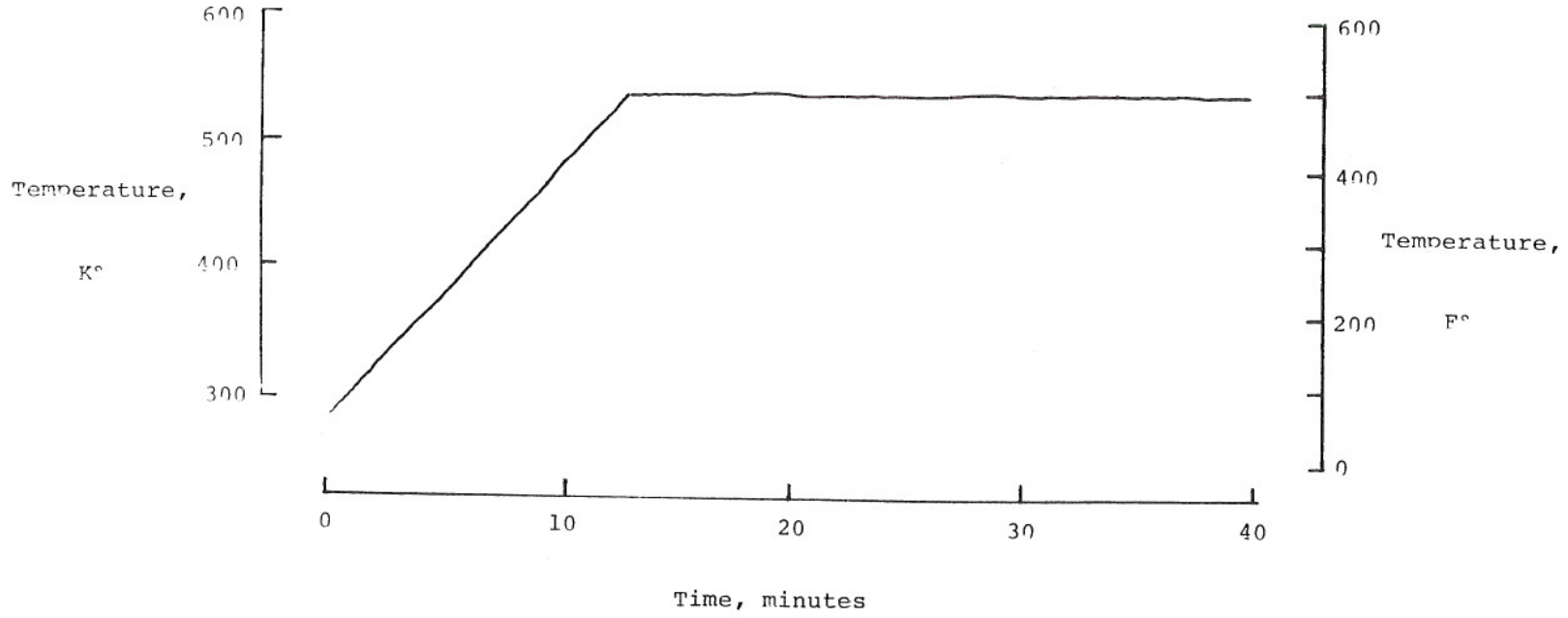

Figure 4. Time-history of temperature applied to the skin of the test specimen.

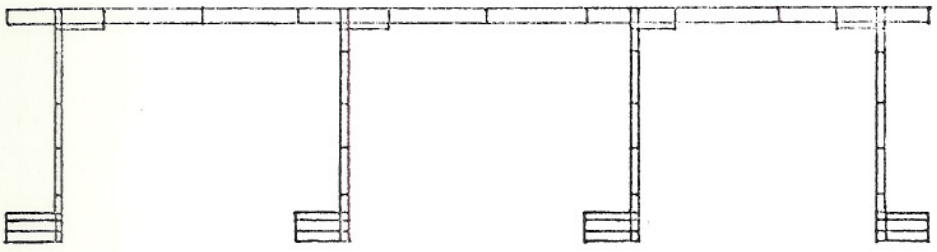

Arrangement of Conduction Elements

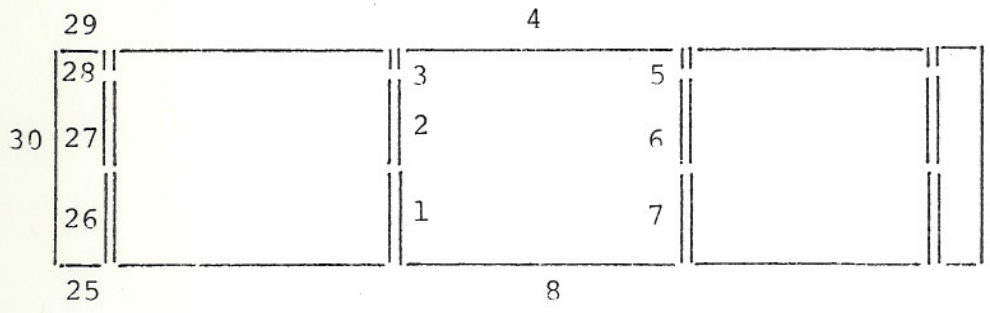

Arrangement of Radiation Elements

Figure 5. Configuration of the thermal model.

i \ j	1	2	3	4	5	6	7	8
1	.0							
2	.0	.0						
3	.0	.0	.0					
4	3.58	5.76	1.96	.0				
5	.74	.93	.24	1.33	.0			
6	2.03	2.40	.52	5.41	.0	.0		
7	2.34	2.08	.40	3.33	.0	.0	.0	
8	6.40	4.32	.84	21.64	.64	4.00	6.24	.0

i \ j	25	26	27	28	29	30
25	.0					
26	2.39	.0				
27	.46	.0	.0			
28	.23	.0	.0	.0		
29	.68	.64	1.76	1.38	.0	
30	3.27	8.00	13.44	2.10	2.87	.0

Figure 6. Typical elements of the view factor matrix input to the NASTRAN radiation model.

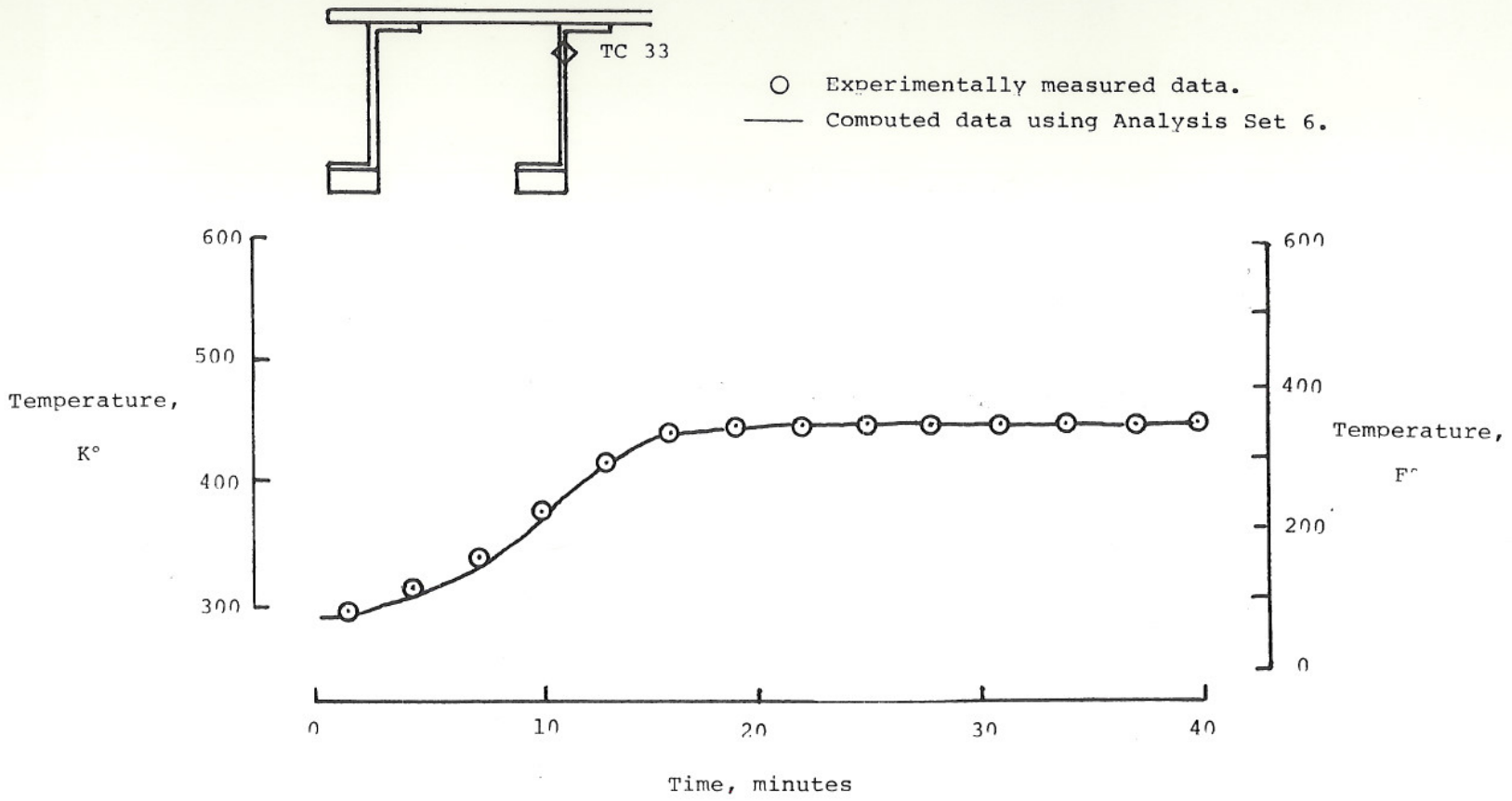

(a) Thermocouple 33.

Figure 7. Comparison of time-histories of calculated and computed spar temperatures.

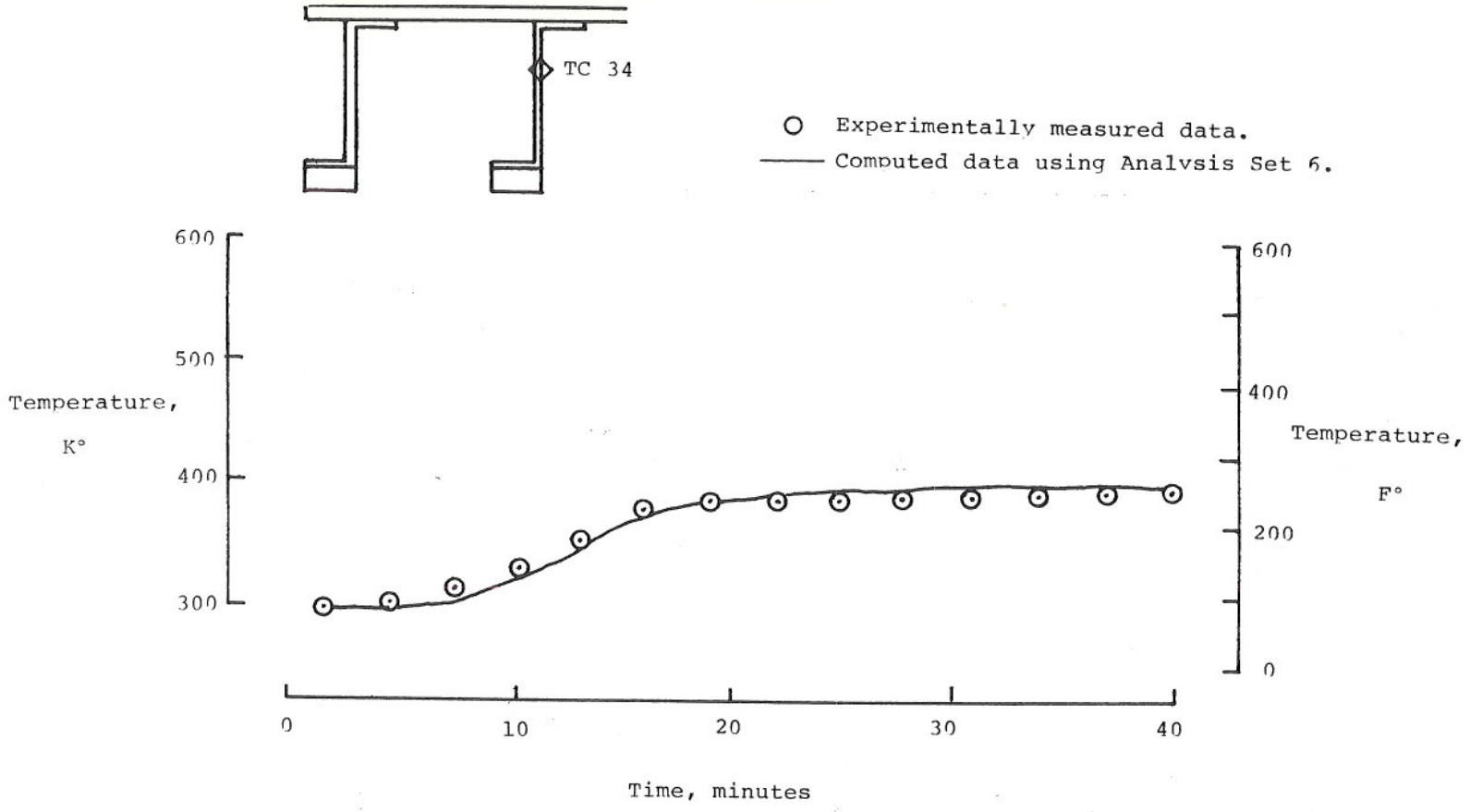

(b) Thermocouple 34.

Figure 7. Continued.

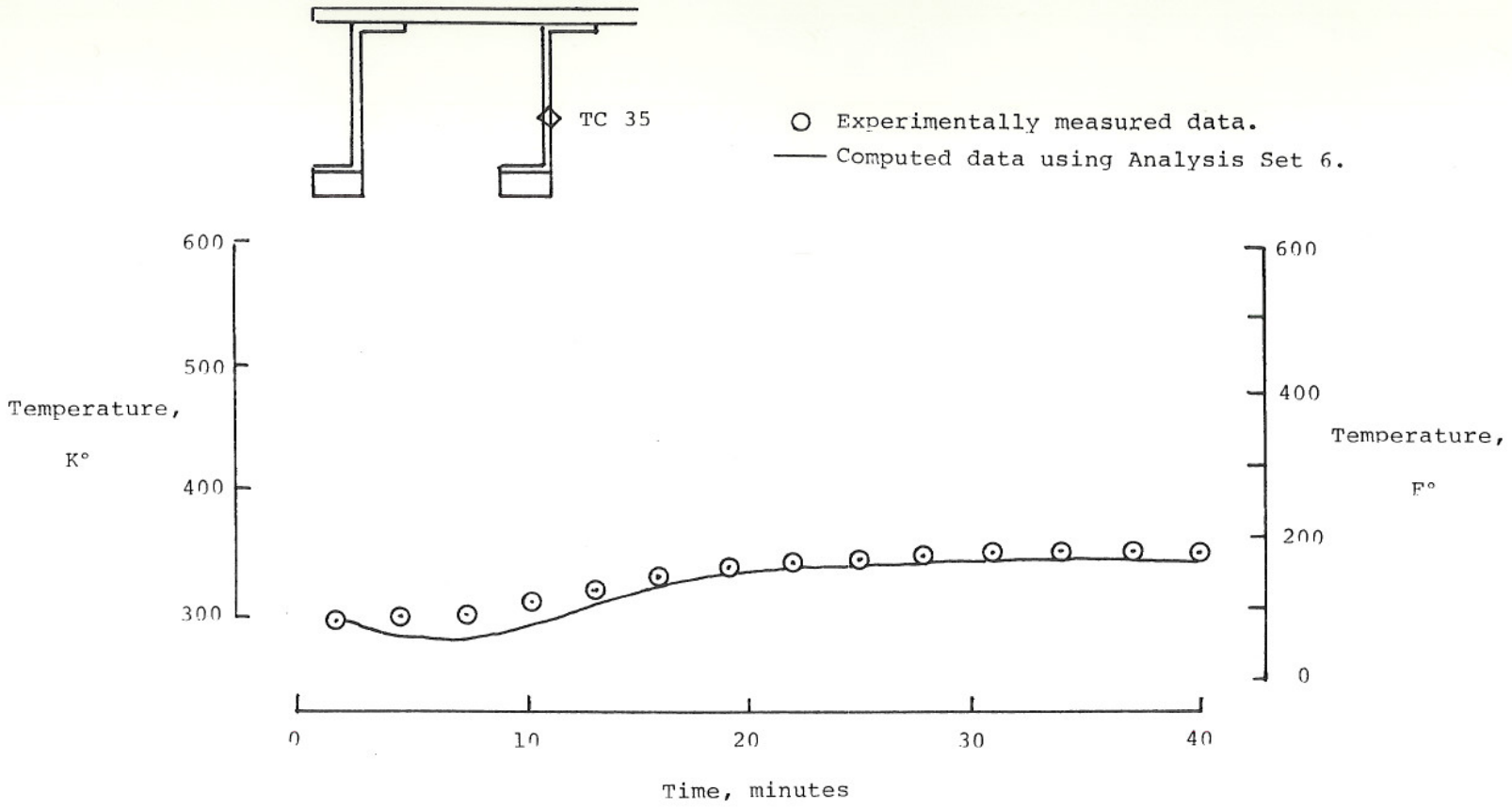

(c) Thermocouple 35.

Figure 7. Continued.

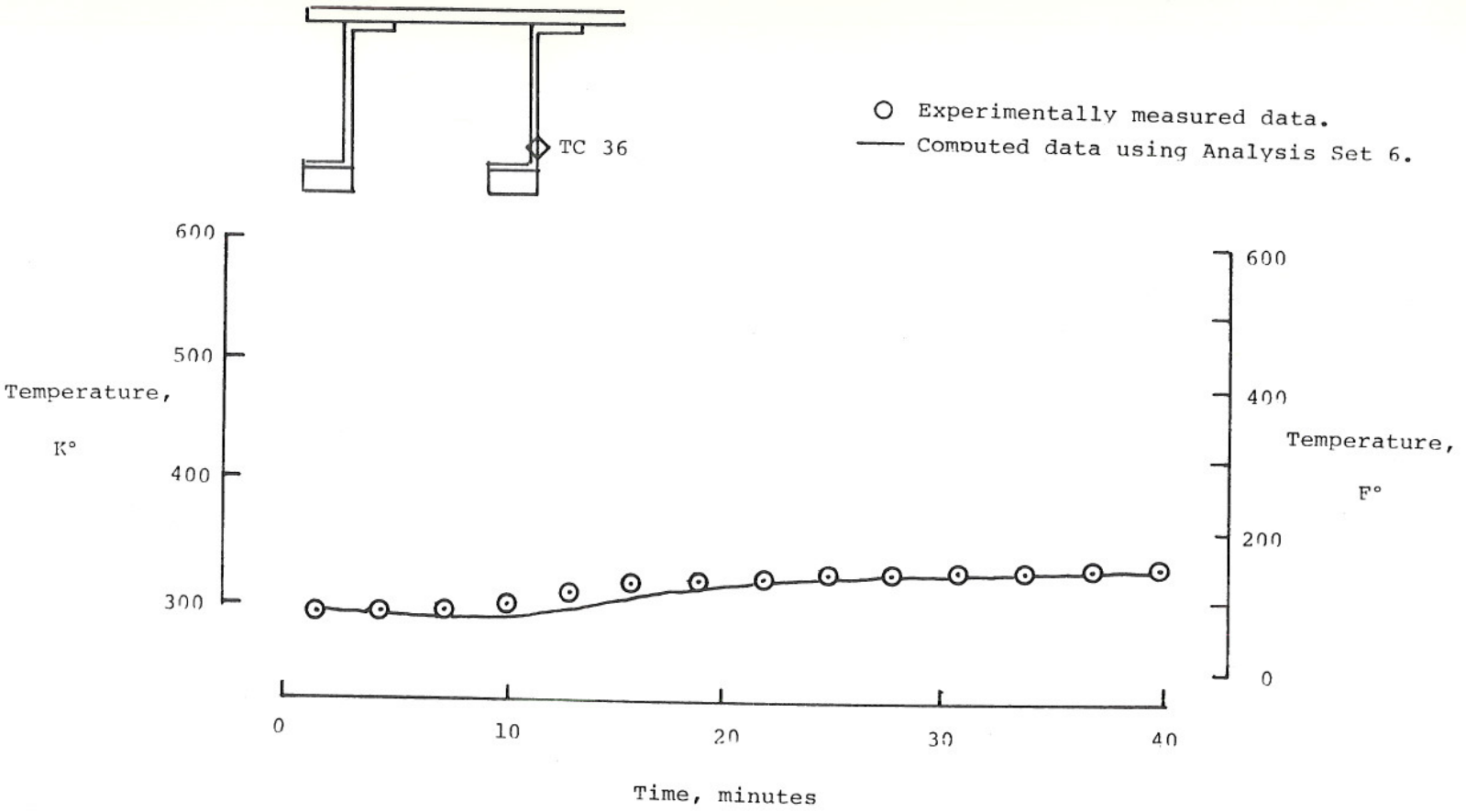

(d) Thermocouple 36.

Figure 7. Continued.

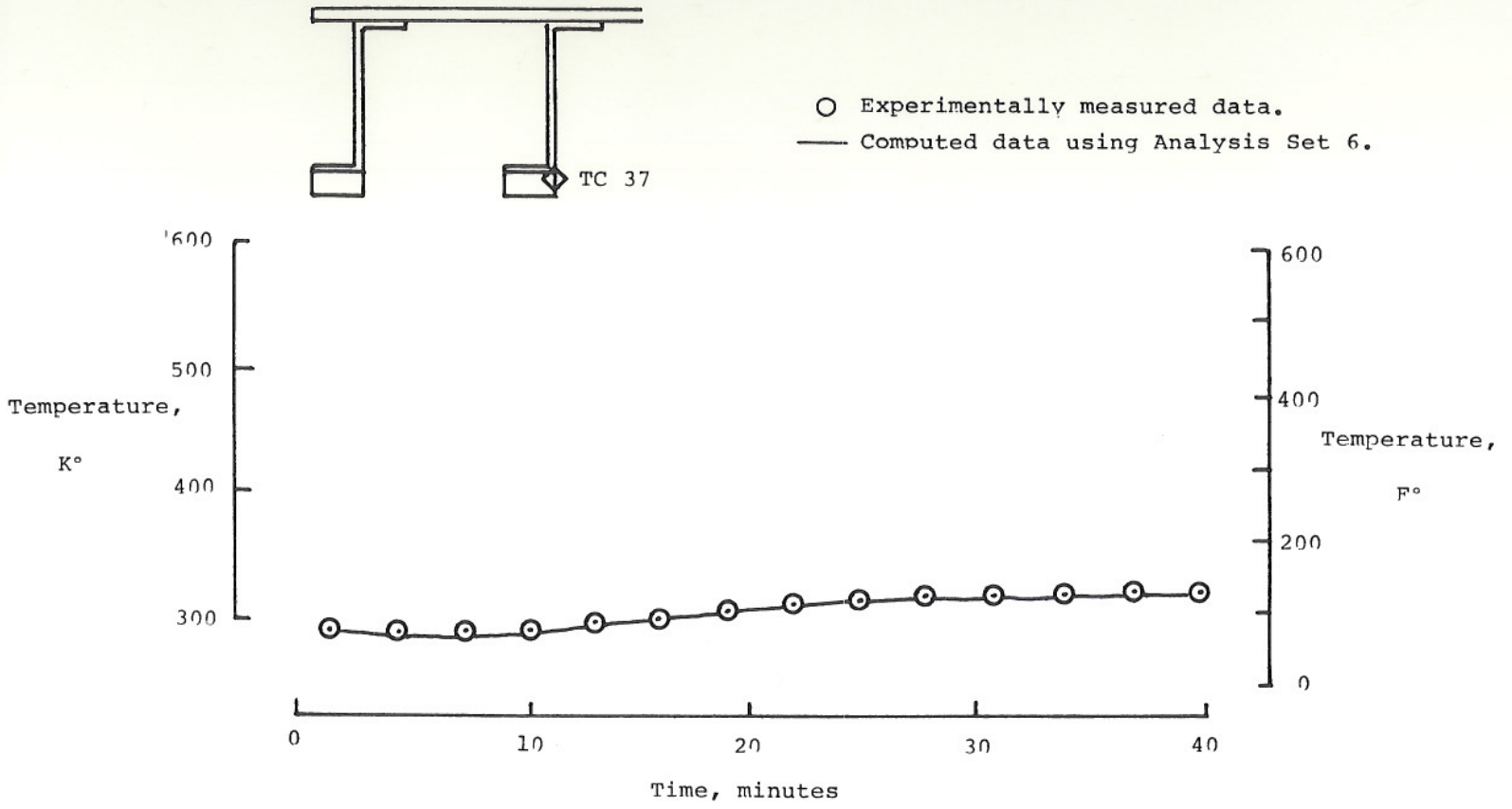

(e) Thermocouple 37.

Figure 7. Concluded.

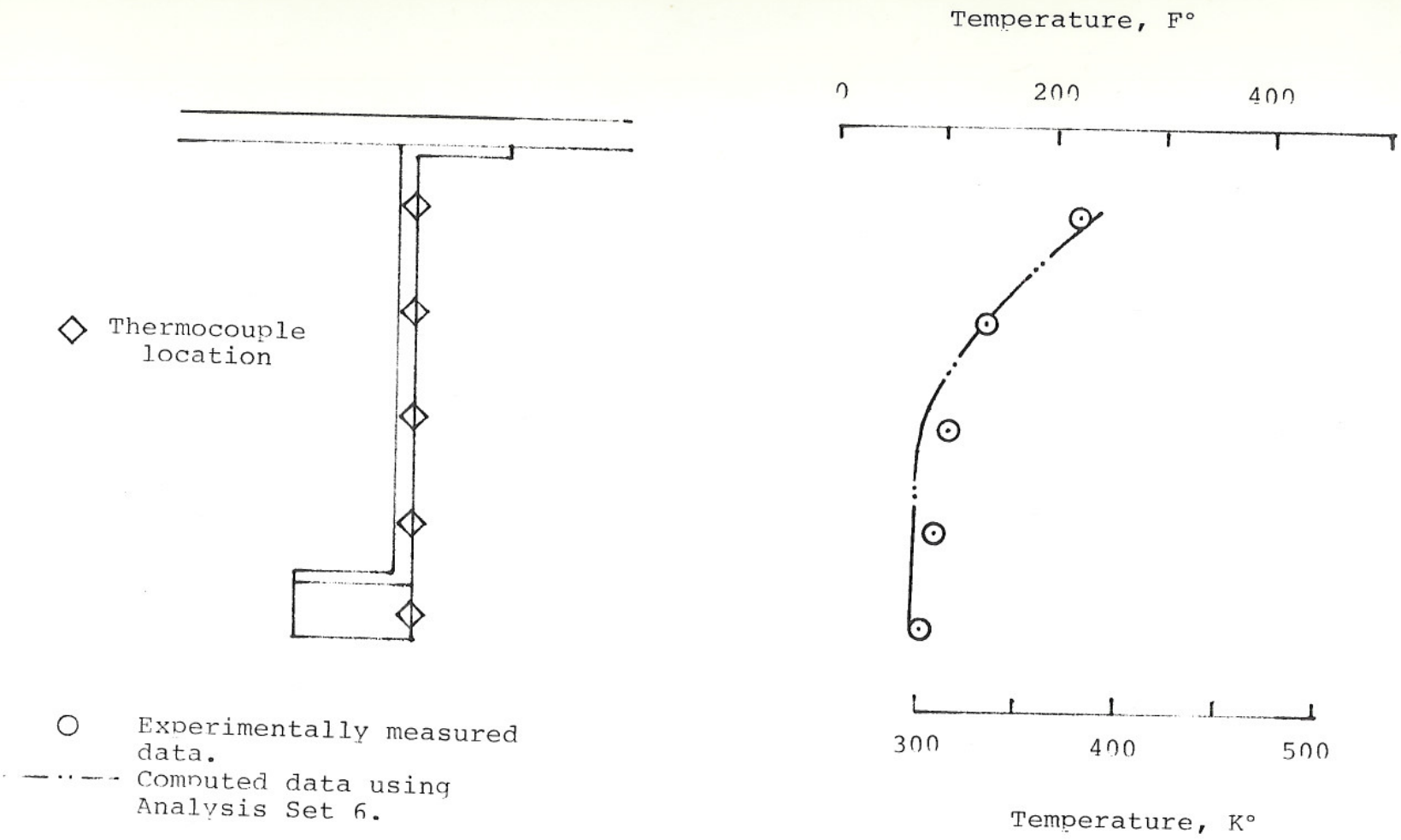

(a) Time = 10 minutes.

Figure 8. Comparison of experimentally measured spar temperatures with computed values.

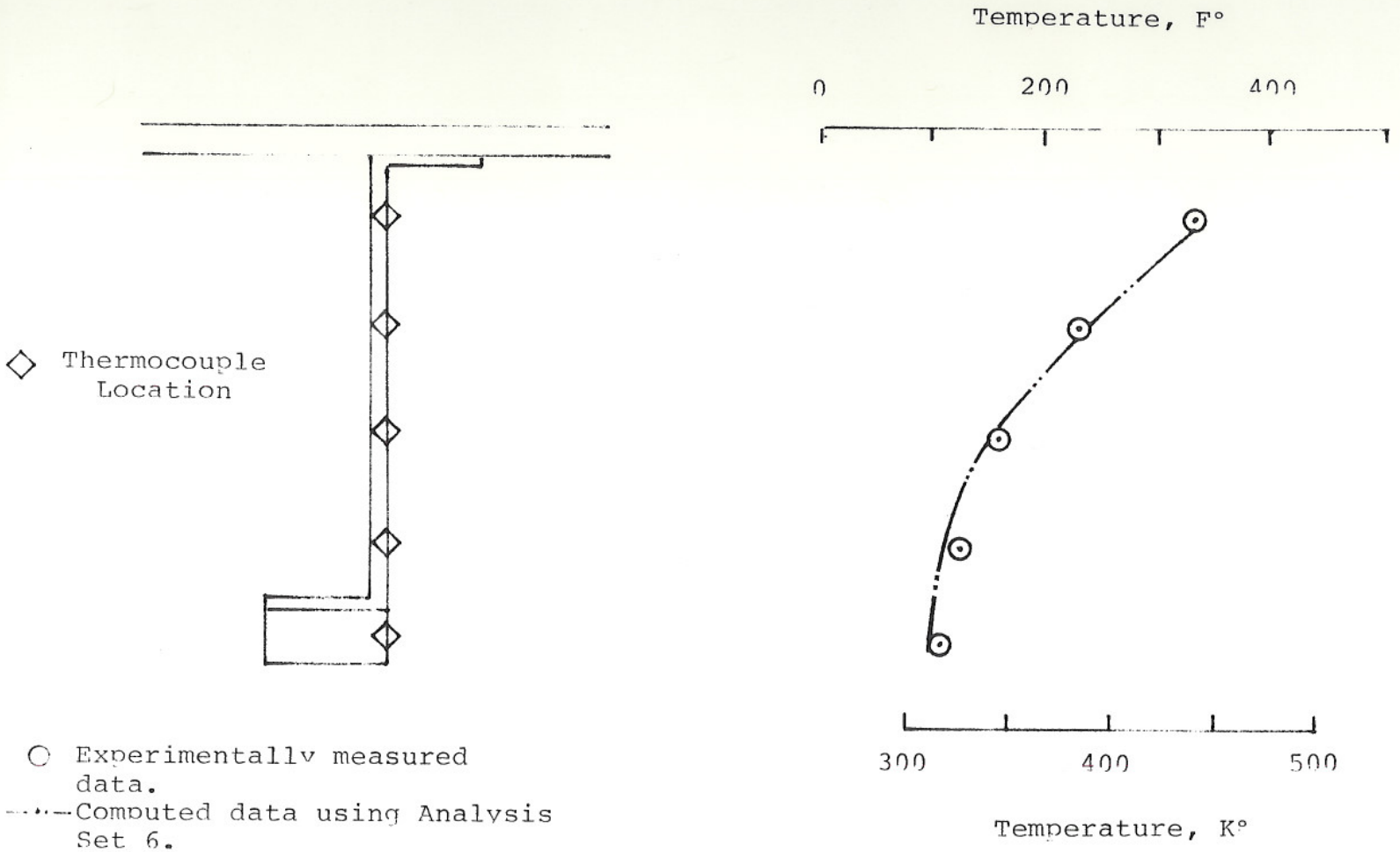

(b) Time = 20 minutes.

Figure 8. Continued.

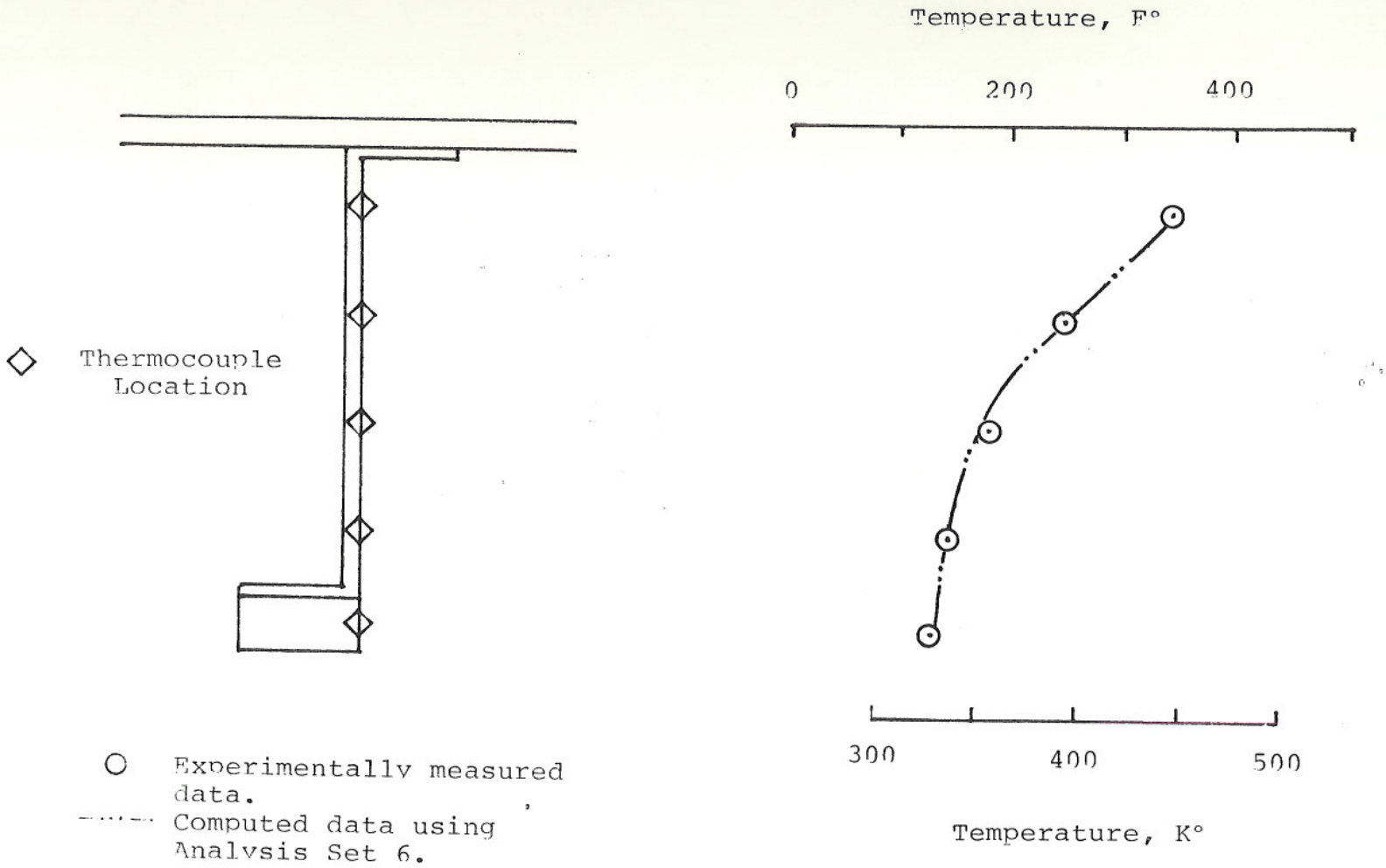

(c) Time = 40 minutes.

Figure 8. Concluded.

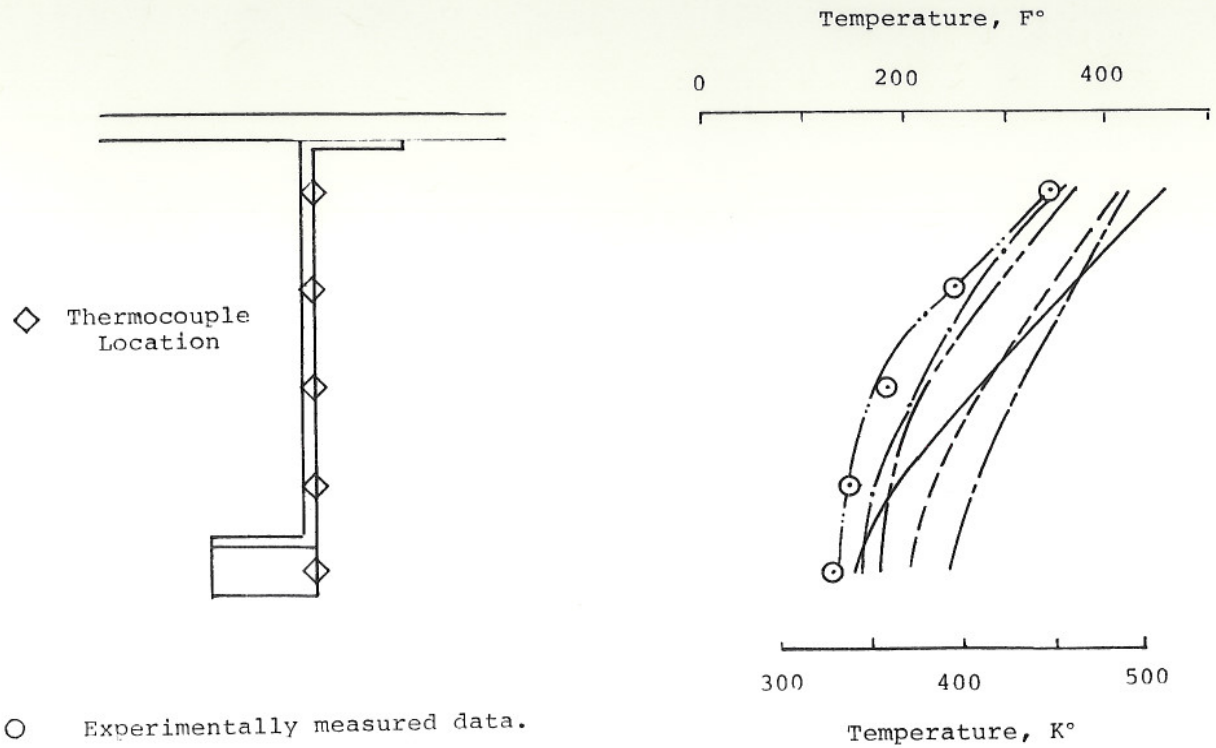

○ Experimentally measured data.

——— Analysis Set 1, Conduction, no radiation, no convection.
— — — Analysis Set 2, Conduction, free radiation, ε = .9, no convection.
— - — Analysis Set 3, Conduction, solid closure plates, ε = .9, no convection.
— — — Analysis Set 4, Conduction, solid closure plates, ε = .9, small film coefficient.
— · — Analysis Set 5, Conduction, solid closure plates, ε = .9, large film coefficient.
— ·· — Analysis Set 6, Conduction, solid closure plates, ε = .64, large film coefficient.

Figure 9. Comparison of measured temperatures with calculated values for several analysis variations at time equals forty minutes.

1. Report No.	2. Government Accession No.	3. Recipient's Catalog No.
NASA TM-81359		

4. Title and Subtitle	5. Report Date
A Comparison of Laboratory Measured Temperatures With Predictions for a Spar/Skin Type Aircraft Structure	6. Performing Organization Code RTOP 506-53-64

7. Author(s)	8. Performing Organization Report No.
Jerald M. Jenkins	10. Work Unit No.

9. Performing Organization Name and Address	11. Contract or Grant No.
Dryden Flight Research Center P.O. Box 273 Edwards, California 93523	13. Type of Report and Period Covered Technical Memorandum

12. Sponsoring Agency Name and Address	14. Sponsoring Agency Code
National Aeronautics and Space Administration Washington, D.C. 20546	

15. Supplementary Notes

16. Abstract

A typical spar/skin aircraft structure was heated non-uniformly in a laboratory and the resulting temperatures were measured. The heat transfer function of the NASTRAN computer program was used to provide predictions. The measured and calculated data were compared. Calculated temperatures based on a thermal model with conduction, radiation, and convection features compared closely to measured spar temperatures. Acceptable results were obtained without varying the thermal conductivity, specific heat, or emissivity with temperature since the range of temperature variations was not large. All modes of heat transfer (conduction, radiation, and convection) were shown to significantly affect the magnitude and distribution of structural temperatures.

17. Key Words (Suggested by Author(s))	18. Distribution Statement
Heat transfer Hypersonic structures	Unclassified - Unlimited STAR category 05

19. Security Classif. (of this report)	20. Security Classif. (of this page)	21. No. of Pages	22. Price*
Unclassified	Unclassified	23	A02

*For sale by the National Technical Information Service, Springfield, VA 22161